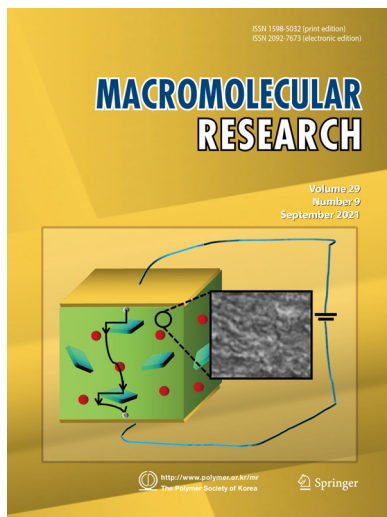


COVER PAPER

Lowering Dielectric Loss and AC Conductivity of Polymer/HfC Composite Dielectric Films via Insulating Montmorillonite Barrier

Peiyao Chen, Binghe Chen, Ben Qin, Jiangqiong Wang, Qihuang Deng*, and Yefeng Feng*

Vol. 29, No. 9, pp 589–596 (2021) | SEP 25, 2021 | DOI 10.1007/s13233-021-9076-6



Highly conductive HfC ceramic filler shows robust interfacial polarization with P(VDF-HFP) matrix, resulting in the elevated high dielectric constant in ternary composite films. Highly insulative montmorillonite ceramic filler exhibits rather weak ability of charge transmission, leading to the reduced conductive ability and dielectric loss in ternary composite films. The hindered transfer of charge carriers from polymer/HfC interfacial zone can be triggered by montmorillonite particles, leading to the greatly decreased leakage current in ternary composites.

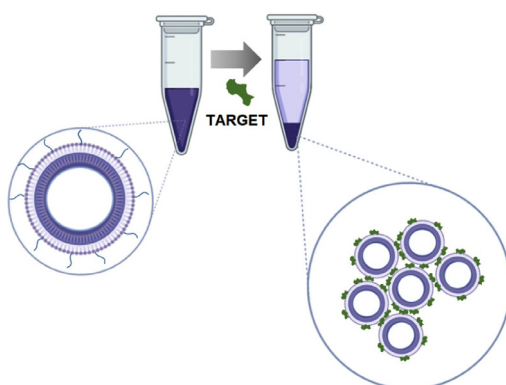
COMMUNICATION

Self-Assembled Peptide-Labeled Probes for Agglutination-Based Sensing

Anura Shrestha, Butaek Lim,
Priyanka Shiveshwarkar,
Gumaro Rojas, Izele Abure,
Anthony David Nelson,
and Justyn Jaworski*

Macromol. Res., 29, 577 (2021)

Diacetylene amphiphiles produced with functionalized peptide based recognition moieties for a target of interest were self-assembled and polymerized. The polydiacetylene vesicles bearing target specific peptides were capable of serving as an agglutination-based probe when placed in the presence of a multivalent target capable of binding the peptide displayed on the probe. The binary sensing approach was demonstrated as functional across a broad dynamic range relevant to immune profiling.



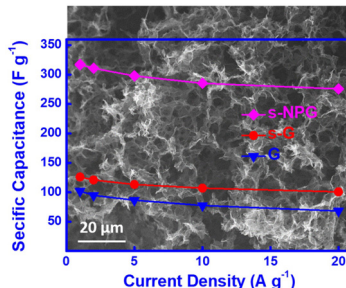
ARTICLES

Improved Pseudocapacitive Performance of Graphene Architectures Modulating by Nitrogen/Phosphorus Dual-Doping and Steam-Activation

Chaonan Wang, Junhong Zhao,
Shengyun Luo, and Xu Yu*

Macromol. Res., **29**, 582 (2021)

Steam-assistant nitrogen and phosphorus dual-doped graphene architecture (s-NPG) exhibits highly porous structure and the wrinkled surface. The pyridinic-N and C-P-O bonds as the dominant active sites are formed after steam-activation treatment. By the effect of hierarchical structure and the surface modification, s-NPG shows the improved pseudocapacitive behavior, like high specific capacitance, good rate capability and cyclic stability.

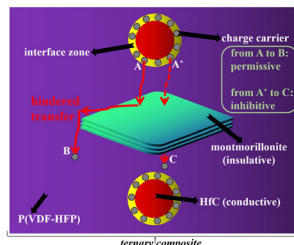


Lowering Dielectric Loss and AC Conductivity of Polymer/HfC Composite Dielectric Films via Insulating Montmorillonite Barrier

Peiyao Chen, Binghe Chen, Ben Qin,
Jiangqiong Wang, Qihuang Deng*,
and Yefeng Feng*

Macromol. Res., **29**, 589 (2021)

Highly conductive hafnium carbide (HfC) ceramic filler shows robust interfacial polarization with poly(vinylidene fluoride-hexafluoropropylene) (P(VDF-HFP)) matrix, resulting in the elevated high dielectric constant in ternary composite films. Highly insulative montmorillonite ceramic filler exhibits rather weak ability of charge transmission, leading to the reduced conductive ability and dielectric loss in ternary composite films. The hindered transfer of charge carriers from polymer/HfC interfacial zone can be triggered by montmorillonite particles, leading to the greatly decreased leakage current in ternary composites.



Reinforcing Efficiency of Pyrolyzed Spent Coffee Ground in Styrene-Butadiene Rubber

Supparoek Boopasiri,
Ponghorn Sae-Oui, Sirilug Lundee,
Sukanya Takaewnoi,
and Chomsri Siriwong*

Macromol. Res., **29**, 597 (2021)

This research aimed to study the reinforcing efficiency of pyrolyzed spent coffee ground (SCG) in styrene-butadiene rubber (SBR). The SCG was initially treated at elevated temperatures of 700 °C and 900 °C (under nitrogen gas) before being characterized by various techniques, e.g., particle size analysis, Fourier transform infrared spectroscopy, X-ray diffraction and scanning electron microscopy. After being added into SBR, properties of the rubber compounds and vulcanizates were determined. The results showed that pyrolysis of SCG at 700 °C and 900 °C significantly reduced the average particle size from 39.8 μm to 27.3 μm and 25.3 μm, respectively. The addition of pyrolyzed SCG into SBR resulted in the increases of both rubber-filler interaction, as evidenced from the increase of bound rubber content, and crosslink density, leading to the improvement of mechanical properties of the rubber vulcanizates when compared with the addition of untreated SCG.

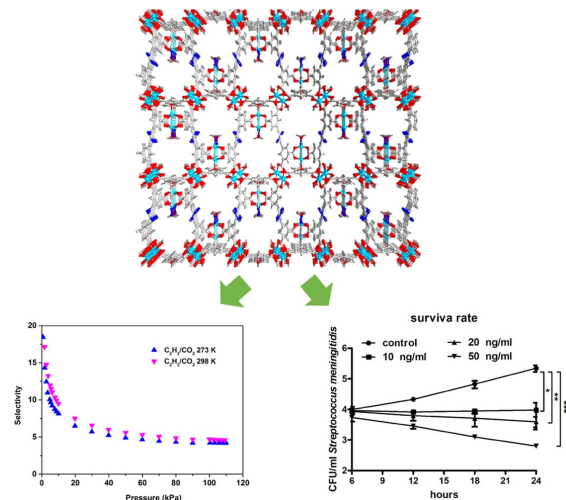


Porous Zn(II)-Organic Framework with Tetrazolyl Decorated Pores for Selective C₂H₂ Adsorption and Treatment Activity on Infantile Meningitis

Yang Yu, Qi-Gai Yin*, Li-Jing Ye, and Hui Yu

Macromol. Res., **29**, 605 (2021)

A new Zn(II)-containing metal-organic framework has been successfully prepared, and its activated sample holds a relative large C₂H₂ sorption capacity of 164.0 cm³ (STP) g⁻¹ at 298 K and 1 bar with the C₂H₂/CH₄ and C₂H₂/CO₂ sorption selectivity of 34.8 and 4.6 at 298 K, respectively. Additionally, we studied its application value on the infantile meningitis as well as the related mechanism was evaluated.

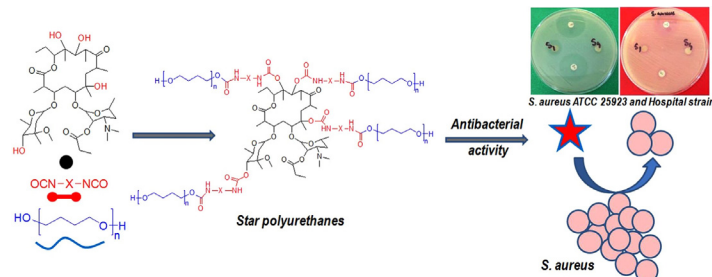


Synthesis, Characterization of Erythromycin Propionate Core-Based Star Poly(ether urethane)s and Their Antibacterial Properties

Daniela Filip*, Doina Macocinschi, Cristina Gabriela Tuchilus, Mirela Fernanda Zaltariov, and Cristian Dragos Varganici

Macromol. Res., **29**, 613 (2021)

New four-arm star poly(ether urethanes) (star PUs) based on erythromycin propionate core, toluene 2,4-diisocyanate and 4,4'-methylenebis(phenyl isocyanate) as diisocyanates and Terathane of different molecular weights as polyether arms are prepared to investigate their structure-property relationship. These star PUs reveal antibacterial properties and therefore they can be used as antibacterial biomaterials.

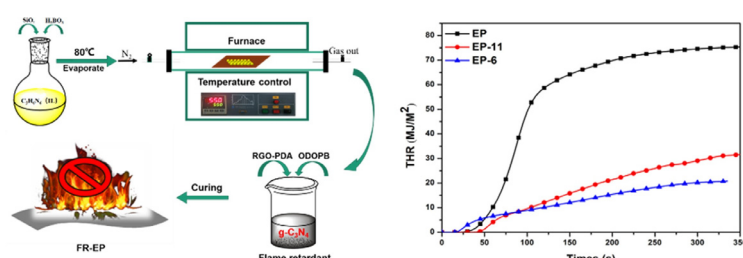


Flame Retardancy of Epoxy Resin Improved by Graphene Hybrid Containing Phosphorous, Boron, Nitrogen and Silicon Elements

Li Li, Huan Wang, Fenglin Hua, Mingming Wang, Yuanshuo Zhang, Hui Xi, Jing Yang, Zhiwang Yang*, and Ziqiang Lei*

Macromol. Res., **29**, 625 (2021)

An effective ternary organic-inorganic composite flame retardant of reduced graphene oxide-poly-dopamine graphitic carbon nitride@10-(2,5-dihydroxyphenyl)-10-H-9-oxa-10-phospho-phenanthrene-10-oxide (RGO-PDA@g-C₃N₄@ODOPB) was successfully fabricated and applied to enhance the flame retardancy of epoxy resin. The incorporation of RGO-PDA@g-C₃N₄@ODOPB resulted in the increase of char yield, 20% adding of RGO-PDA@g-C₃N₄@ODOPB/ammonium polyphosphate (APP) led to the decreasing of the peak heat release rate and the total heat release at 78% and 62.5%, respectively. Meanwhile, the limit oxygen index value of the epoxy resin (EP) composites was as high as 29% and reached UL-94 V-0 rate.

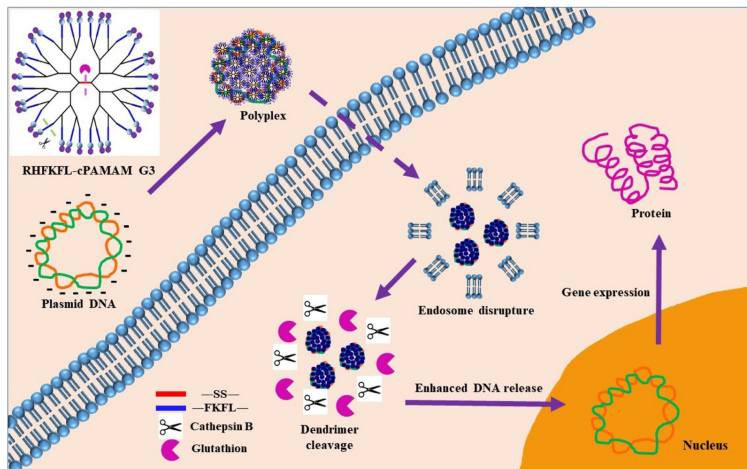


Synthesis and Characterization of Dual-Sensitive PAMAM Derivatives Conjugated with Enzyme Cleavable Peptides as Gene Carriers

Jeil Lee, Seunghye Park,
Yong-Eun Kwon, Eugeney Oh,
Dong Woon Kim, Hwanuk Guim,
Jehyeong Yeon, Jin-Cheol Kim,
and Joon Sig Choi*

Macromol. Res., **29**, 636 (2021)

In this study, we selected cystamine core polyamidoamine (PAMAM) generation 3 (cPAMAM G3), a bioreducible polymer, and synthesized the FKFL sequence, as a cathepsin B-cleavable linker to cPAMAM G3. In addition, we simultaneously introduced RH dipeptides to RHFKFL-cPAMAM G3 to improve transfection efficiency. The synthesized RHFKFL-cPAMAM G3 showed similar transfection efficiency and low cytotoxicity compared with that of PEI 25 kDa in HepG2 and SW480 cells, which are cathepsin B enzyme overexpression cell lines. These results imply that a combination of enzyme- and reduction-responsive linkers can be used to solve the problems associated with the use of nonviral vectors.

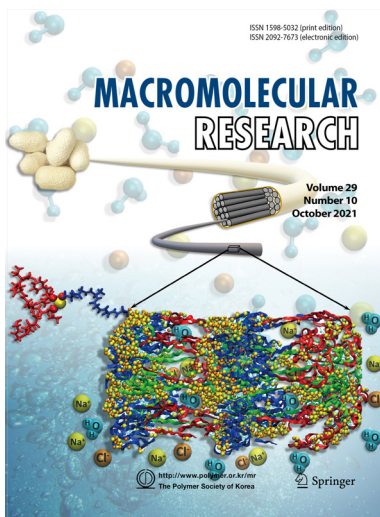


COVER PAPER

Insights into Nanomechanical Behavior and Molecular Mechanisms in *Bombyx Mori* Silk Fibroin in Saline Environment Using Molecular Dynamics Analysis

Mrinal Patel, Devendra K. Dubey*, and Satinder Paul Singh

Vol. 29, No. 10, pp 694–712 (2021) | OCT 25, 2021 | DOI 10.1007/s13233-021-9084-6



B. mori SF being a prospective biomaterial, entails the understanding of effect of saline environment on mechanical behaviour and nanoscale mechanics of *B. mori* SF. Enhanced mechanical response of *B. mori* SF nanostructure is observed with increase in salt concentrations. This enhanced mechanical response is attributed to peptide–salt interatomic interactions, predominantly by forming peptide–salt–peptide ionic bridges.

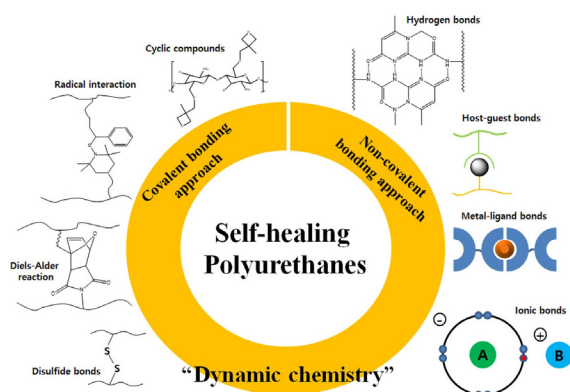
REVIEWS

A Brief Review of Self-Healing Polyurethane Based on Dynamic Chemistry

Won-Ji Lee, Hyeon-Gyeong Oh,
and Sang-Ho Cha*

Macromol. Res., **29**, 649 (2021)

Polyurethanes, known for their durability, excellent mechanical characteristics, are applied for various applications. When the materials are suffered by external energy, self-healable material can autonomously restore its original properties. The intrinsic self-healing is categorized into two types including reversible covalent bonds and reversible non-covalent bonds. Self-healing polyurethanes not only improve their reliability but also extend material's service life time.

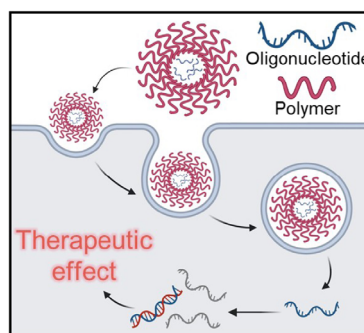


Systematic Combination of Oligonucleotides and Synthetic Polymers for Advanced Therapeutic Applications

Moohyun Han, Jiyun Beon,
Ju Young Lee, and Seung Soo Oh*

Macromol. Res., **29**, 665 (2021)

The potential of oligonucleotides is exceptional in therapeutics compared to conventional therapeutic agents. However, many obstacles have hampered their clinical success. Use of polymeric carriers can be an effective approach for overcoming the biological barriers and thereby maximizing the therapeutic efficacy of the oligonucleotides. In this review, we presented a variety of systematic combinations between the therapeutic oligonucleotides and the synthetic polymers.

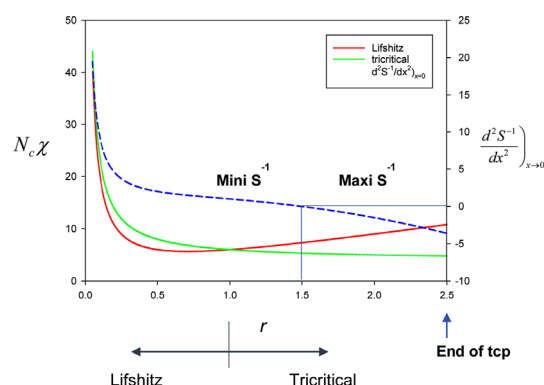


Classical Critical Behaviors and Ginzburg Criteria for Polymer Mixtures

Junhan Cho*

Macromol. Res., **29**, 681 (2021)

Critical lines for a ternary blend of A, B homopolymers of the same sizes and symmetric A-B diblock copolymer, where the segregation strength $N_c\chi$ at isotropic Lifshitz critical points and tricritical points along with the isotropic Lifshitz tricritical point as a crossover is drawn as a function of chain size ratio r of homopolymer to copolymer. The valid regions for those multicritical points are also displayed.



ARTICLES

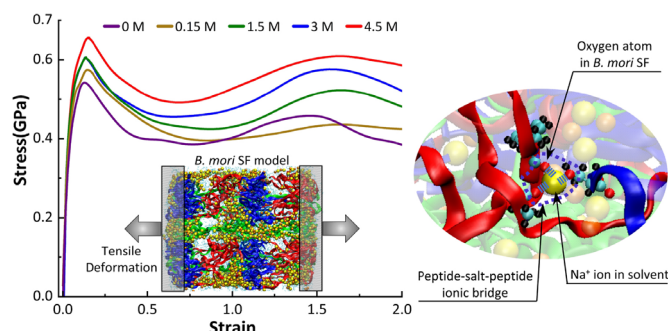
Insights into Nanomechanical Behavior and Molecular Mechanisms in *Bombyx Mori* Silk Fibroin in Saline Environment Using Molecular Dynamics Analysis

Mrinal Patel, Devendra K. Dubey*,
and Satinder Paul Singh

Macromol. Res., **29**, 694 (2021)

Cover Paper

Bombyx mori silk fibroin (*B. mori* SF) being a prospective biomaterial, entails the understanding of effect of saline environment on mechanical behaviour and nanoscale mechanics of *B. mori* SF. Enhanced mechanical response of *B. mori* SF nanostructure is observed with increase in salt concentrations. This enhanced mechanical response is attributed to peptide–salt–peptide ionic bridges, predominantly by forming peptide–salt–peptide ionic bridges.

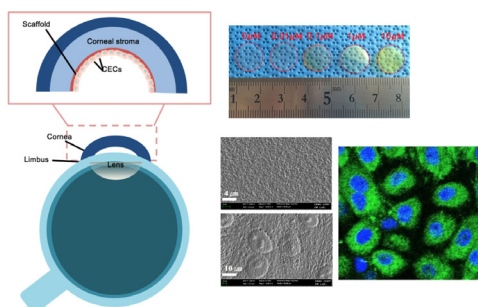


Enhanced Silk Fibroin-Based Film Scaffold Using Curcumin for Corneal Endothelial Cell Regeneration

Do Kyung Kim, Sanghyuk Lee,
Joo Hee Choi, Bo Sung Jung,
Ki Soo Kim, Jeong Eun Song,
Rui L. Reis, and Gilson Khang*

Macromol. Res., **29**, 713 (2021)

Constructing bioengineered cornea to replace cornea transplant is a challenge. Silk fibroin (SF)-based film scaffold has been applied as a promising tool for cornea tissue engineering. SF has great biocompatibility, biodegradability, and physical properties. In order to enhance the mechanical characters, biological property, and anti-inflammatory effect of the SF, curcumin (CC) was incorporated in this study. The mechanical characterization and in vitro study with rabbit-derived cornea endothelial cells (rCECs) were performed to confirm applicability and potential of CC/SF film scaffold.

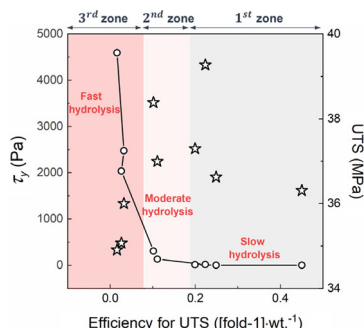


Rheological Percolation of Cellulose Nanocrystals in Biodegradable Poly(butylene succinate) Nanocomposites: A Novel Approach for Tailoring the Mechanical and Hydrolytic Properties

Hyo Jeong Kim, Yun Hyeong Choi,
Ji Hun Jeong, Hyeri Kim,
Ho Sung Yang, Sung Yeon Hwang,
Jun Mo Koo*, and Youngho Eom*

Macromol. Res., **29**, 720 (2021)

Biodegradable nanocomposites of poly(butylene succinate) (PBS) and cellulose nanocrystals (CNCs) (0.2–3.0 wt%) were fabricated, and their mechanical and hydrolytic properties were tailored based on a rheological strategy. The PBS-CNC nanocomposites exhibited two rheological percolation thresholds at 0.8 and 1.5 wt%. Interestingly, the trend changes of mechanical and hydrolytic properties were observed at the thresholds. Therefore, this study offers a rheological basis to control the performances of the biodegradable nanocomposites.

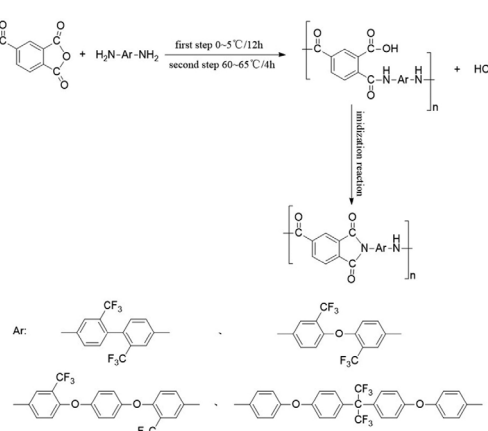


Study on Preparation and Properties of PAI Materials Containing Trifluoromethyl in Side Chain

Haiyang Yang, Duxin Li*, Jun Yang*,
Jin Wang, Shunchang Gan,
Kaikai Cao, and Yufeng Liu

Macromol. Res., **29**, 727 (2021)

In this paper, diamine monomers containing trifluoromethyl in the side chain were selected to design the molecular structure of polyamide-imide (PAI), and materials were prepared by the acyl chloride method. The effects of diamine monomer containing fluorine were studied to prepare PAI materials with good heat resistance, excellent friction and wear properties, and low water absorption.



Carbazole-Based Polyimide as a Hole-Transporting Material for Optoelectronic Applications

Thi Kieu Trang Tu,
Sabrina Aufar Salma, Mijin Jeong,
Joo Hyun Kim, Yeon Tae Jeong,
Yeong-Soo Gal,
and Kwon Taek Lim*

Macromol. Res., **29**, 735 (2021)

A novel carbazole-based polyimide is prepared and studied as a potential hole-transporting material. The carbazole-based polyimide is found to have high thermal and morphological stabilities, reasonable highest occupied molecular orbital (HOMO)-lowest unoccupied molecular orbital (LUMO) energy levels, and acceptable hole mobility, which suggests that it is a promising material for optoelectronic applications.

